Enhancement of the conductivity of Ba2In2O5 through phosphate doping

Shin, Jaegil; Hussey, L; Orera, Alodia; Slater, Peter

DOI:
10.1039/C0CC00063A
10.1039/c0cc00063a

Enhancement of the conductivity of $Ba_2In_2O_5$ through phosphate doping

J. Felix Shin[a], Laura Hussey[b], Alodia Orera[a] and Peter R. Slater[a*]

[a]School of Chemistry, University of Birmingham, Birmingham. B15 2TT. UK
[b]Chemical Sciences, University of Surrey, Guildford, Surrey, GU2 7XH, UK

In this paper, we demonstrate the successful incorporation of phosphate into $Ba_2In_2O_5$, which leads to the conversion from an orthorhombic to a cubic unit cell. The resulting increased oxygen vacancy disorder leads to an enhancement in the oxide ion conductivity at low temperatures. In addition, in wet atmospheres, significant proton conduction is observed.

Solid Oxide Fuel Cells (SOFCs) are attracting considerable interest as next generation energy conversion devices due to their high efficiencies and accompanying low emissions. For the electrolyte in such devices, a material displaying either high oxide ion conductivity or proton conductivity at elevated temperatures is required, with the main focus of research in this field being materials with the fluorite or perovskite structures[1-3]. One of the most well known perovskite-related oxide ion conductors is $Ba_2In_2O_5$, whose oxide ion conductivity is closely linked to its crystal structure[4,5]. At room temperature, it adopts an orthorhombic brownmillerite-type structure (figure 1) containing ordered oxide ion vacancies, leading to alternating layers of InO_6 octahedra and InO_4 tetrahedra. As a result of this ordering of the oxide ion vacancies, the oxide ion conductivity is comparatively low. At a temperature of ≈ 930 °C, there is a phase change from orthorhombic to tetragonal resulting in disordering of these oxygen vacancies, and a corresponding discontinuous jump in oxide ion conductivity by more than an order of magnitude[4,5]. At higher temperature still, above 1040 °C, the cell becomes cubic, as the oxide ion vacancies become completely disordered[5].

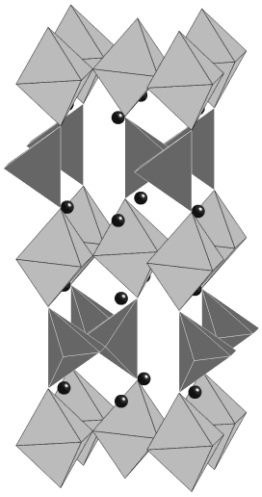

Figure 1. The brownmillerite structure adopted by $Ba_2In_2O_5$, showing alternating layers of InO_6 and InO_4 units

Like other oxygen deficient perovskite related materials, $Ba_2In_2O_5$ will also incorporate water into the oxide ion vacancies at low temperatures in wet atmospheres, according to equation 1

$$V_O^{\bullet\bullet} + O_O + H_2O \leftrightarrow 2\ OH_O^{\bullet} \qquad (1)$$

This hydration (up to 1 mole H_2O per formula unit) leads to the formation of a tetragonal phase, and the observation of significant proton conduction.[6,7] In addition, at low temperatures, a p-type contribution to the conductivity is observed in oxidising atmospheres due to oxygen incorporation according to equation 2.

$$V_O^{\bullet\bullet} + ½\ O_2 \leftrightarrow O_O + 2h^{\bullet} \qquad (2)$$

As a result of the high oxide ion conductivity in the high temperature disordered phase of $Ba_2In_2O_5$, there have been many studies into doping strategies on the In site to stabilise this phase to lower temperatures. Isovalent doping studies have shown that the transition temperature can be lowered by the incorporation of ions with smaller ionic radii than In.[8] However, by far the most successful strategy, has proved to be doping with higher valent cations, such as Sn,[9] Ti,[10] V, Mo

and W [11] . Other attempts to stabilise the highly conducting phase to lower temperatures have included doping on the Ba site with Sr or La[12,13]. There are, however, concerns regarding the long term stabilities of these doped systems, and therefore we have investigated an alternative doping strategy. Our approach stems from previous work on the incorporation of oxyanions into perovskite-type cuprate superconductors. This work showed that perovskite systems could incorporate significant levels of oxyanions (carbonate, nitrate, sulphate, phosphate)[14-19], and moreover such a doping strategy could be used to stabilise phases, which could not be formed without doping; e.g. the Sr analogue of the high temperature superconductor, $YBa_2Cu_3O_{7-x}$. [16]
In this study, we have therefore investigated the possibility of doping phosphate anions onto the In site in $Ba_2In_2O_5$, with the aim of reducing the basicity of the system and hence improving long term stability. We here demonstrate the successful incorporation of phosphate, along with a corresponding enhancement in the conductivity.

High purity $BaCO_3$, In_2O_3 and $NH_4H_2PO_4$ were used to prepare $Ba_2In_{2-x}P_xO_{5+x}$ (x = 0, 0.1, 0.2, 0.3) samples. A 3% excess of $BaCO_3$ was employed to overcome Ba loss at elevated temperatures. Without this small Ba excess, low levels of Ba deficient impurity phases, such as $BaIn_2O_4$ and $Ba_4In_6O_{13}$, were observed after sintering, as has been seen in other studies synthesising similar Ba containing phases.[20, 21] The ground powders were first heated to 1000 °C for 12h. They were then ball-milled (350 rpm for 1 hour, Fritsch Pulverisette 7 Planetary Mill) and reheated to 1000 °C for a further 50h. The products were then pressed as pellets (1.3 cm diameter) and sintered at 1300 °C for 10h. The pellets were covered in sample powder and the crucible was covered with a lid to limit the amount of Ba loss during the sintering process. The phase purity was determined by powder X-ray diffraction (Bruker D8 diffractometer with Cu $K\alpha_1$ radiation). In order to provide further evidence for the successful incorporation of phosphate, Raman spectroscopy measurements were made using a Renishaw inVia Raman microscope with excitation using a Cobolt Samba CW 532 nm DPSS Laser.
For the conductivity measurements, sintered pellets (>84% theoretical density) were coated with Pt paste, and then heated to 750°C for 1 hour to ensure bonding to the pellet. Bulk conductivities were then measured by AC impedance measurements (Hewlett Packard 4182A impedance analyser) in the range from 0.1 to 10^3 kHz. Measurements were made in dry N_2 to eliminate the p-type contribution to the conductivity. In addition measurements were made in wet N_2 (in which the gas was bubbled at room temperature through water) to identify any protonic contribution to the conductivity.
In order to gather information regarding the effect of phosphate doping on water incorporation, powder samples were heated to 800 °C in wet N_2, and then slow cooled (0.4 °C/min) to room temperature to allow sample hydration. The water content of the hydrated samples were then analysed using thermogravimetric analysis (Netsch STA 449 F1 Jupiter Thermal Analyser). Samples were heated at 10 °C/min to 1000 °C in N_2.

X-ray diffraction data confirmed the successful synthesis of single phase samples of $Ba_2In_{2-x}P_xO_{5+x}$ in the range $0 \leq x \leq 0.3$. X-ray diffraction patterns for x=0, 0.1, 0.3, are shown in figure 2.

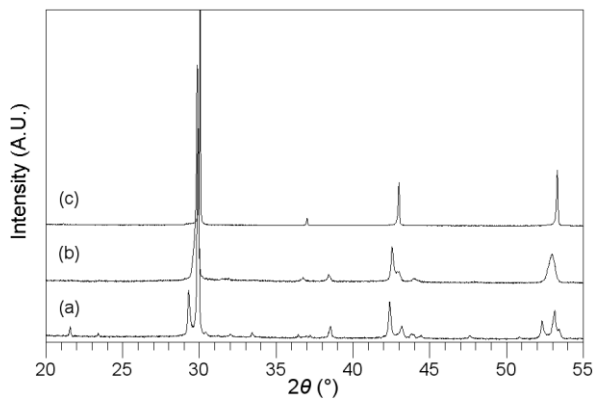

Figure 2. . X-ray diffraction patterns for $Ba_2In_{2-x}P_xO_{5+x}$, (a) x=0, (b) x= 0.1, (c) x=0.3.

These XRD data showed a change from orthorhombic – tetragonal – cubic as the phosphate content increased. Moreover, the cell volume was shown to decrease with increasing phosphate content, in line with the smaller size of P^{5+} versus In^{3+} (figure 3).

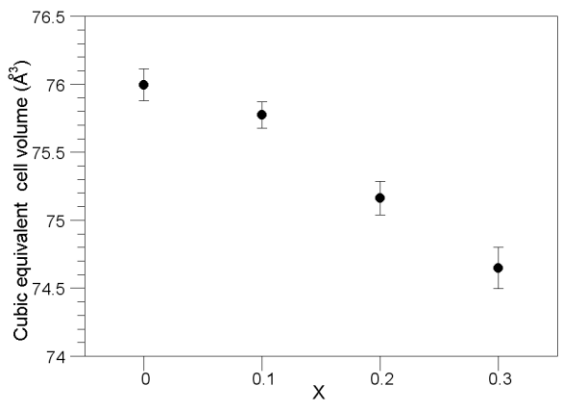

Figure 3. Variation of equivalent cell volume with phosphate content for $Ba_2In_{2-x}P_xO_{5+x}$.

Two factors could be accounting for the change in cell symmetry

1. The effect of the smaller size of PO_4^{3-} compared to InO_4^{5-}, which disrupts the oxygen vacancy ordering.
2. The higher charge of P compared to In leading to an increase in the oxide ion content. A similar stabilisation of the cubic cell is seen on Sn doping for In, which also leads to an increase in oxygen content[8].

Further evidence for the successful incorporation of phosphate was provided by Raman spectroscopy studies, which showed a reduction in the intensity of the In-O bands, and the emergence of bands due to phosphate (figure 4).

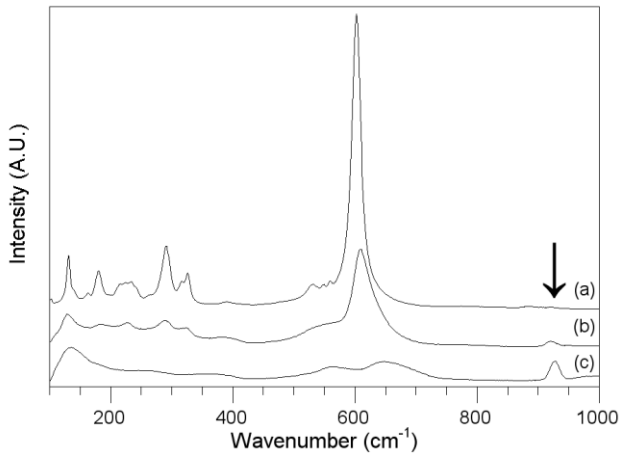

Figure 4. Raman spectra for $Ba_2In_{2-x}P_xO_{5+x}$, (a) x=0, (b) x= 0.1, (c) x=0.3, showing the emergence of peaks due to the presence of phosphate.

Following the demonstration of the successful incorporation of phosphate, the effect of this doping strategy on the conductivity was examined. Figure 5 shows the conductivity data for the x=0.0, 0.1, and 0.3 samples. As can be seen from these data, the low temperature conductivity is significantly enhanced on increasing phosphate doping. This can explained by the disordering of the oxygen sublattice. At higher temperatures, the conductivity for x=0.1 is, however, higher than that for x=0.3. This increase in conductivity at higher temperatures for x=0.1, can be related to the elevated temperature introducing disordering of the oxide ion vacancies in this phase, supported by preliminary high temperature X-ray diffraction studies. The fact that in the disordered region the conductivity for x=0.1 is greater than x=0.3 would suggest a small degree of vacancy defect trapping on phosphate doping. Evidence for this can also be provided by comparing conductivities at 790°C for samples with varying phosphate content (figure 6).

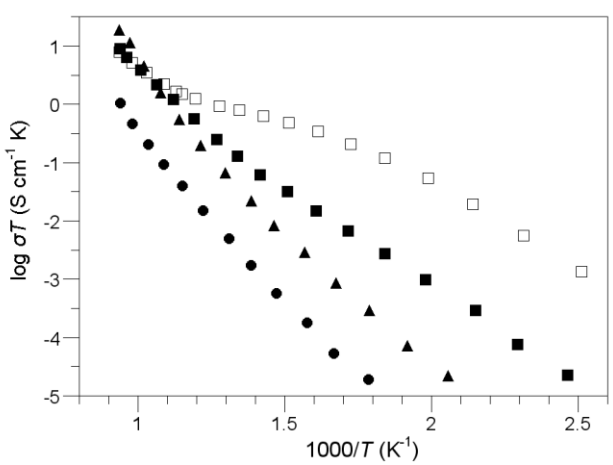

Figure 5. Conductivity data in dry N_2 for $Ba_2In_{2-x}P_xO_{5+x}$, x=0 (filled circles), x=0.1 (filled triangles), x=0.3 (filled squares). Conductivity data in wet N_2 for x=0.3 also shown (open squares)

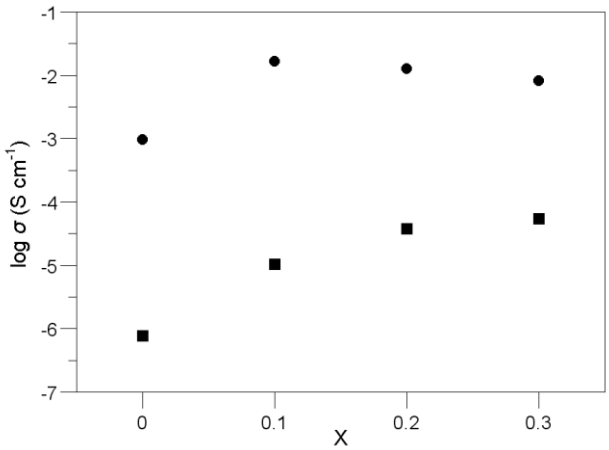

Figure 6. Variation in σ_{790} (filled circles) and σ_{400} (filled squares) in dry N_2 with phosphate content, x, in $Ba_2In_{2-x}P_xO_{5+x}$. Data show an enhancement in the low temperature conductivity with increasing phosphate content, while at high temperatures there is an initial enhancement, followed by a small conductivity decrease for higher phosphate contents.

In addition to the high oxide ion conductivity, there was also evidence for significant proton conductivity in wet atmospheres, as illustrated by an enhancement in the conductivity (figure 5, σ_{400C}=7.7 x 10^{-4} Scm^{-1} in wet N_2). This proton conductivity originates from water incorporation into the oxide ion vacancies according to equation 1. The degree of water uptake in these samples was investigated by thermogravimetric analysis. These experiments indicated that as phosphate is doped into the sample, the maximum water content achievable decreases (e.g. water content decreases from 1 mole to 0.4 mole per formula unit from x=0 to x=0.3) This can be partly explained by the increase in starting oxide ion content, meaning there are less oxide ion vacancies to fill. However, the decrease in water content is higher than might have been expected given the starting oxide ion content, e.g. for $Ba_2In_{1.7}P_{0.3}O_{5.3}$, a water content of 0.7 H_2O, to fill all the vacant oxide ion sites, might have been predicted. The observation of a lower water content (0.4 H_2O) can be explained by the tetrahedral coordination of P (in the phosphate ion), which hence precludes the filling of the other two vacant sites in the perovskite B site coordination sphere around it.

Further detailed studies are required to investigate the structural influence of the phosphate in more detail. Preliminary structural refinement for X-ray diffraction data of the highest P content sample (x=0.3) provides confirmation of P incorporation, with In and P contents of 1.68(4) and 0.32(4) respectively, in agreement with those expected. Further neutron diffraction studies are, however, planned to investigate the structural features in more detail. In addition, further studies are planned to investigate the long term stability of these phosphate doped phases.

In summary, we have demonstrated that phosphate can be doped into $Ba_2In_2O_5$, leading to the introduction of disorder on the oxygen sublattice, and hence an increase in oxide ion conductivity, as well as significant proton conductivity in wet atmospheres. The work shows the potential for oxyanion doping as a novel strategy to enhance the oxide ion/proton conductivity of fuel cell electrolytes. Further preliminary studies have shown that sulphate doping is similarly successful in this respect.

Notes and references

1. K. D. Kreuer, *Annu. Rev. Mater. Res.*, 2003**, 33**, 333.
2. J. B. Goodenough, *Annu. Rev. Mater. Res.* 2003, **33**, 91.
3. A. Orera, P.R. Slater; *Chem. Mater*. 2010, **22**, 675.

4. J. B. Goodenough, J. E. Ruizdiaz, Y. S. Zhen, *Solid State Ionics*, 1990**, 44**, 21.
5. S. A. Speakman, J. W. Richardson, B. J. Mitchell, S. T. Misture, *Solid State Ionics*, 2002**, 149**, 247.
6. G. B. Zhang, D. M. Smyth, *Solid State Ionics*, 1995**, 82**, 153.
7. T. Schober, J. Friedrich, F. Krug, *Solid State Ionics*, 1997**, 99**, 9.
8. T. Q. Ta, T. Tsuji, Y. Yamamura, *J. Alloys and Cpdss*, 2006**, 408**, 253.
9. T. Schober, *Solid State Ionics*, 1998**, 109**, 1.
10. V. Jayaraman, A. Magrez, M. Caldes, O. Joubert, M. Ganne, Y. Piffard, L. Brohan, *Solid State Ionics*, 2004**, 170**, 17.
11. A. Rolle, R. N. Vannier, N. V. Giridharan, F. Abraham, *Solid State Ionics*, 2005**, 176**, 2095.
12. K. Kakinuma, H. Yamamura, H. Haneda, T. Atake, *Solid State Ionics*, 2001**, 140**, 301.
13. H. Yamamura, Y. Yamada, T. Mori, T. Atake, *Solid State Ionics*, 1998**, 108**, 377.
14. C. Greaves and P. R. Slater, *J. Mater. Chem.*, 1991, **1**, 17.
15. C. Greaves and P. R. Slater, *Physica C*, 1991, **175**, 172.
16. P. R. Slater, C. Greaves, M. Slaski, C. M. Muirhead, *Physica C*, 1993, **208**, 193.
17. Y. Miyazaki, H. Yamane, N. Ohnishi, T. Kajitani, K. Hiraga, Y. Morii, S. Funahashi, T. Hirai; *Physica C*, 1992, **198**, 7.
18. A. Maignan, M. Hervieu, C. Michel, B. Raveau ; *Physica C*, 1993, **208**, 116.
19. K. Kinochita, T. Yamada; *Nature* 1992, **357**, 313.
20. T. Omata, T. Fuke, S. Otsuka-Yao-Matsuo, *Solid State Ionics*, 2006**, 177**, 2447.
21. A. M. Abakumov, M. D. Rossell, O. Y. Gutnikova, O. A. Drozhzhin, L. S. Leonova, Y. A. Dobrovolsky, S. Y. Istomin, G. Van Tendeloo, E. V. Antipov, *Chem. Mate.*, 2008**, 20**, 4457

We would also like to express thanks to the University of Birmingham for funding (EPS international studentship for JFS). The Bruker D8 diffractometer, Netsch Thermal analyser, and Renishaw inVia Raman microscope used in this research were obtained through the Science City Advanced Materials project: Creating and Characterising Next generation Advanced Materials project, with support from Advantage West Midlands (AWM) and part funded by the European Regional Development Fund (ERDF)